ISSN 0029-3865

CBPF-NF-062/88

MOLECULAR ORBITAL CALCULATIONS OF THE UNPAIRED ELECTRON DISTRIBUTION AND ELECTRIC FIELD GRADIENTS IN DIVALENT PARAMAGNETIC Ir COMPLEXES

by

S.R. NOGUEIRA*, N.V. VUGMAN* and Diana GUENZBURGER+

+Centro Brasileiro de Pesquisas Físicas - CBPF/CNPq
Rua Dr. Xavier Sigaud, 150
22290 - Rio de Janeiro, RJ - Brasil

*Universidade Federal do Rio de Janeiro - UFRJ
Instituto de Física
Cidade Universitária - Ilha do Fundão
21945 - Rio de Janeiro, RJ - Brasil

ABSTRACT

Semi-empirical Molecular Orbital calculations were performed for the paramagnetic complex ions $[Ir(CN)_5]^{3-}$, $[Ir(CN)_5C\ell]^{4-}$ and $[Ir(CN)_4C\ell_2]^{4-}$. Energy levels schemes and Mulliken-type populations were obtained. The distribution of the unpaired spin over the atoms in the complexes was derived, and compared to data obtained from Electron Paramagnetic Resonance spectra with the aid of a Ligand Field model. The electric field gradients at the Ir nucleus were calculated and compared to experiment. The results are discussed in terms of the chemical bonds formed by Ir and the ligands.

Key-words: Ir complexes; Molecular orbital; Electric field gradient.

1 INTRODUCTION

There has been considerable interest in the electronic structure and spectroscopic properties of the transition metal cyanide complexes. Some of these complexes are diamagnetic but can be made paramagnetic by capturing electrons produced by irradiation with X-rays. The metal ions in the irradiated complexes may show unusual and unstable oxidation states and their properties can be investigated by Electron Paramagnetic Resonance (EPR)[1].

We have been interested in the EPR of transition metal hexacyanide complexes inserted in alkali halide host lattices for the past several years[2]-[7]. Alkali halides have been the most fancied host crystals for incorporating the transition metal complexes in diluted and isolated form for the EPR studies. This has been possible because of the good matching of the symmetry and size of several transition metal cyanide complexes with several appropriate alkali halide lattices.

The measured EPR spectra reveals the presence of several d^7 low spin paramagnetic species in irradiated crystals. The species can be divided into three categories i.e. pentacyano/hexacyano, mono-and dichlorinated species[2].

The spin-Hamiltonian used to interpret the EPR spectra includes an electronic Zeeman interaction (effective spin S=1/2), a hyperfine interaction between the electron magnetic moment and the magnetic moments of nuclei with non-null nuclear spin, and a quadrupolar interaction between the nuclear quadrupole moment of the metal ion and the electric field gradient (EFG) at the nuclear site. Additional terms including nuclear Zeeman interactions are ignored, as their first order contribution to the spectra are usually small enough to be neglected.

Usually quadrupolar interactions are not detected in EPR spectra, as they are much smaller than magnetic hyperfine interactions. However, when a nucleus combines a small magnetogyric ratio and a rather large nuclear quadrupole moment and is located in a site with a non-null EFG, the quadrupole term in the spin - Hamiltonian can be of the same order of magnitude as the magnetic hyperfine one. EPR spectra then become very unusual, and the quadrupolar interaction can be accurately measured, as is the case for divalent iridium and monovalent osmium complexes[7].

We will focus on the divalent Iridium Cyanide complexes that are formed by irradiation of $[Ir(CN)_6]^{3-}$ in alkali chloride host lattices, namely $[Ir(CN)_5]^{3-}$, $[Ir(CN)_5C\ell]^{4-}$ and $[Ir(CN)_4C\ell_2]^{4-}$. For these species, we obtained the spin distribution on the different atoms from the measured spin-Hamiltonian parameters accordingly to a Ligand Field model, described below, which has been extensively used in the literature[8]; EFG values were taken directly from the measured quadrupolar interactions.

For the purpose of interpreting this experimentally - derived data in terms of the chemical bonding within the complex ions, we have performed semi-empirical Molecular Orbital (MO) calculations for the species above, thus obtaining the general characteristics of their electronic structure. The distribution, in terms of Mulliken-type populations, of the unpaired electron over the atoms of the complexes was derived and compared to the corresponding EPR data. We also obtained the electric field gradients at the Ir nucleus for the three complexes; these calculated values were compared to the experimental values, and the relative importance of the 5d and 6p contributions to the EFG was assessed, as well as the influence of the Ir-Cℓ bond distance in the complexes $[Ir(CN)_5C\ell]^{4-}$

and $[Ir(CN)_4C\ell_2]^{4-}$.

In Section 2 we describe the Ligand Field model which was employed to derive the unpaired electron distribution from the EPR data; in Section 3 we describe the Molecular Orbital method; in Section 4 are given the results obtained with the MO calculations and compared to the experimental parameters; finally, in section 5 we give a summary of the main conclusions drawn.

2 THE LIGAND FIELD MODEL

For a C_{4v} or D_{4h} symmetry low spin system the unpaired electron occupies a d_{z^2} orbital ($^2A_1$ on $^2A_{1g}$ ground state). Spin-orbit coupling causes the admixture of the ground state configuration with the ^2E state from excited configurations (only the first one is usually considered in the calculations). The $|E'\alpha'>$ components of the Kramer's doublet for these two configurations, in the complementary scheme, are $|b_1^2a_1^+>$ and $|a_1^2(1)^->$, respectively.

In the Ligand Field model, the atomic d orbital is allowed to mix with the ligand orbitals, so the corresponding orbitals can be written

$$a_1 = \alpha\tilde{a}_1 - \alpha'\Psi_{a_1} \quad \text{and} \quad (1) = \beta(\tilde{1}) - \beta'\Psi_{L_1}$$

where $\tilde{a}_1$ is the $5d_{z^2}$ orbital with mixing coefficient α and (1) the partner in the Kramer's doublet; Ψ_{a_1} and Ψ_{L_1} are linear combinations of the ligand orbitals of appropriate symmetry. The symbol "~" indicates an atomic orbital.

After diagonalization of the spin-orbit interaction matrix and evaluation of the components of the g and A tensors[3] we get

$$g_{\parallel} = g_0\cos2\theta + 2k'' \sin^2\theta \quad (1)$$

$$g_{\perp} = g_0\cos^2\theta + \sqrt{6}k'\sin2\theta \quad (2)$$

$$A_{\parallel} = [-\kappa + \frac{4}{7}\alpha^2\cos^2\theta + \frac{12}{7}\beta^2\sin^2\theta + (\sqrt{6}/7)\alpha\beta\sin2\theta]P \quad (3)$$

$$A_{\perp} = [-\kappa - \frac{2}{7}\alpha^2\cos^2\theta - \frac{6}{7}\beta^2\sin^2\theta - \frac{15}{14}\sqrt{6}\alpha\beta\sin2\theta]P \quad (4)$$

k' and k'' are orbital reduction factors defined by the following expressions:

$$k' = \langle(1)|\ell_+|a_1\rangle/\sqrt{6} = \alpha\beta - \alpha\beta' S_e - \alpha'\beta S_{a_1} + (\alpha'\beta'/\sqrt{6})\langle\psi_{L_1}|\ell_+|\psi_{a_1}\rangle$$

$$k'' = \langle(1)|\ell_z|(1)\rangle = 1 - \beta'^2(1-\langle\psi_{L_1}|\ell_z|\psi_{L_1}\rangle)$$

S_e and S_{a_1} are the overlap integrals $\langle(\tilde{1})|\psi_L\rangle$ and $\langle\tilde{a}_1|\psi_{a_1}\rangle$, respectively. The angle θ is such that $\tan2\theta = \frac{\sqrt{6}k'y}{1+yk''/2}$, where $y=\lambda/(E_2-E_1)$, λ is the spin-orbit coupling constant, E_2-E_1 is the energy difference between the two mixing configurations, κ is the isotropic Fermi contact constant and $P=g_0g_n\beta_e\beta_n\langle r^{-3}\rangle$.

The sign of the spin-orbit coupling constant has already been changed to give the right expressions for d^7, not d^3 configuration.

Formulas (1) to (4) are a set of four equations and six unknowns. By changing k'' and β usually from 1.0 to 0.6 the $g_{\parallel}$, $g_{\perp}$, $A_{\parallel}$ and $A_{\perp}$ can be fitted to give the values of the various parameters; this results in an uncertainty which is of the order of the uncertainty introduced by the experimental errors. Only the combination of signs for the hyperfine splitting which gives an accep-

table value of $|\alpha|^2$ is chosen.

The core polarization field per unpaired spin can be calculated from the Fermi contact constant by the relation

$$\chi = -\frac{3}{2}\kappa\langle r^{-3}\rangle \tag{5}$$

The spin densities at the ligands are given by[9]:

$$f_s^L = (A_{\parallel}^L + 2A_{\perp}^L)/(3A_s^{theo}) \tag{6}$$

$$f_p^L = (A_{\parallel}^L - A_{\perp}^L)/(3A_p^{theo}) \tag{7}$$

where $A_s^{theo} = (8\pi/3)g_n\beta_n g_e\beta_e|\Psi_e(0)|^2$ is the hyperfine coupling which would arise from an unpaired electron in a ligand valence-shell s orbital and $A_p^{theo} = (2/5)g_n\beta_n g_e\beta_e\langle r^{-3}\rangle$ is half the coupling constant in the direction of the orbital which would arise from an electron in a valence-shell p orbital[10]. $A_{\parallel}^L$ and $A_{\perp}^L$ are the components of hyperfine coupling tensor with ligand L.

3 THE MOLECULAR ORBITAL METHOD

We have performed Molecular Orbital calculations for the Ir complexes, employing the semi-empirical method put forward by Ballhausen and Gray and described in detail elsewhere[11]. This method is based on the earlier method of Wolfsberg and Helmholz[12] for transition metal complexes, with some improvements added, the most noteworthy being a self-consistency scheme which we describe briefly in what follows, and it may be considered a variant of the method

known as "Extended Hückel". Many properties of transition metal complexes have been successfully studied with this scheme[11]; in particular, this method has been proven useful in investigating the electric field gradients in covalent Ru compounds[13].

The problem consists of solving the secular equations of the variational method:

$$([H]-[E][S])[C] = 0 \tag{8}$$

to obtain the energies and the coefficients of the Molecular Orbitals $\Psi_i(\vec{r})$ expanded on a basis of valence symmetrized atomic orbitals $\chi_j^s(\vec{r})$:

$$\Psi_i(\vec{r}) = \sum_j \chi_j^s(\vec{r}) C_{ji} \tag{9}$$

The diagonal elements of the Hamiltonian matrix are approximated as the Valence Orbital Ionization Potentials (VOIPs), which depend on the charge and configuration of the atom. After each time the secular equations are solved, a Mulliken-type population analysis is performed and 5d, 6s and 6p populations are determined for the central Ir atom. The charge and configuration defined in this way is used to obtain a new set of VOIPs for Ir and construct a new Hamiltonian matrix in Eqs.(8), which are solved again to generate a new set of populations. This procedure is iterated until there is no significant difference between the input Ir configuration used to calculate the VOIPs and the output populations.

For the 3d and 4d transition series, the dependence of the VOIPs on the charge and configuration of the atom may be obtained

from the large amount of available data on atomic spectra[14][15]. However, the situation is quite different for the 5d transition elements, since for these the experimental data is very scarce. For this reason, we have obtained VOIPs for Ir theoretically, by atomic self-consistent relativistic numerical Dirac-Slater calculations, in the local density approximation[16]. The Kohn-Sham-Gaspar local exchange potential was employed[17]. The "transition state" concept[18] was used to define Ionization Potentials. In the "transition state" scheme, the Ionization Potential of an atom in a given configuration is the energy of the orbital from which the ionization occurs, in a self-consistent calculation in which 1/2 electron has been removed from this orbital. These calculations yielded good results, as compared to experimentally derived VOIPs, when applied to the few configurations for which measurements are available. Calculated VOIPs for Ir, obtained in this manner, are given in Table I. Details of the atomic Dirac-Slater calculations, as well as calculated VOIPs for other 5d transition elements, will be given in a forthcoming publication[19]. The use of Ionization Potentials for Ir obtained with relativistic self-consistent atomic calculations ensures that relativistic effects are also being taken into account, although partially and indirectly, in the Molecular Calculations, since the VOIPs are used in the [H] matrix in Eq.8. The relativistic treatment in general gives Ionization Potentials which are higher for the "s" electrons (the orbitals are contracted) and smaller for "d" (the orbitals expand), as compared to non-relativistic calculations. Relativistic calculated VOIPs have been used in other reported semi-empirical MO calculations for molecules containing heavy atoms[20][21].

The energies of orbitals σ(CN), π(CN) and π^*(CN) were taken from

reference (22) and were obtained from ionization potentials and spectroscopic transitions. Atomic energies for Cℓ(3s) and Cℓ(3p) orbitals were taken from Ref.(14); a slightly lower energy is used for the 3p orbital participating in σ MOs.

The non-diagonal elements of the Hamiltonian matrix were approximated as the geometrical average of the diagonal elements

$$H_{ij} = -FG_{ij}(H_{ii}.H_{jj})^{1/2} \qquad (10)$$

in which G_{ij} are group overlap integrals[11] and F is an empirical parameter obtained by approximately fitting the electronic transitions of $[Ir(CN)_6]^{3-}$. Actually the optical spectrum of $[Ir(CN)_6]^{3-}$ is rather limited, since the d → d bands occur at very high energies, being obscured by the high-intensity charge transfer bands[23]. Our adopted values $F_\sigma = 2.4$ and $F_\pi = 2.0$ were obtained by an approximate fit to this spectrum. Atomic analytic Slater-type functions for Ir used in the evaluation of the overlap integrals of matrix [S] were obtained from the literature[24]; for the CN ligands, molecular LCAO functions were employed[22] with atomic "double-ζ" functions for C and N given by Clementi[25]. Cℓ functions used were also "double-ζ" functions of Clementi[25].

The concept of atomic "populations" in a molecule is a very useful one in this context. Here we have adopted a variant of the Mulliken populations[26], in which the overlap population is distributed among the atoms in a bond according to a weight proportional to the atomic coefficients in the MO[27]. This definition is more appropriate for transition metal complexes that have occupied MOs which are antibonding in nature, avoiding spurious "s" and "p" negative populations.

The quadrupole interaction takes place between the quadrupole moment of the nucleus and the electric field gradient produced by the charge anisotropy around the probe nucleus. For the ground state of ^{193}Ir with spin 3/2:

$$\Delta E_Q = \frac{1}{2} e V_{zz} Q \qquad (11)$$

where Q is the nuclear quadrupole moment and V_{zz} is the EFG.

In Molecular Orbital theory we have (in atomic units):

$$\frac{V_{zz}}{e} = \sum_k Z_k \frac{3z_k^2 - r_k^2}{r_k^5} - \sum_i n_i \langle \phi_i | \frac{3z^2 - r^2}{r^5} | \phi_i \rangle \qquad (12)$$

where the first summation is the contribution of the nuclei of charge Z_k surrounding the probe atom, and the second is the electronic contribution, summed over Molecular Orbitals ϕ_i with occupation n_i.

In the present approximation, only the valence electrons are considered to contribute to the EFG, and an approximated form of obtaining the EFG is employed, which consists of calculating q for atomic 5d and 6p orbitals occupied by a number of electrons equal to their Mulliken-type populations obtained from the molecular calculations. In this atomic-like model, the electric field gradient matrix elements are integrated over atomic functions, resulting in the Gaunt coefficients obtained from integration over the angles, multiplied by $\langle r^{-3} \rangle$ values calculated over the atomic radial functions. One has then:

$$\frac{V_{zz}}{e} = \frac{4}{7} \langle r^{-3} \rangle_{5d} [(n_{x^2-y^2} - n_{z^2}) + (n_{xy} - n_{xz(yz)})] + \frac{4}{5} \langle r^{-3} \rangle_{6p} (n_{x(y)} - n_z) \qquad (13)$$

where $n_{x^2-y^2}$, etc., are Mulliken-type populations.

A correction for core polarization effects may be obtained by multiplication by the Sternheimer factor[28]. However, as these were derived for free atoms, we prefer not to employ them here, since there is evidence that they may change considerably in a molecular situation[29].

In extracting the EFG from the quadrupole interaction values (Eq.11) taken from the EPR spectra, it is necessary to have a value for the nuclear quadrupole moment Q of ^{193}Ir. Values reported in the literature, usually derived from atomic hyperfine structure, cluster around +0.7b[30]; we adopt the value +0.78b, cited in the compilation of electric field gradients by Vianden[31]. The radial integrals $\langle r^{-3}\rangle_{5d}$ and $\langle r^{-3}\rangle_{6p}$, which enter the evaluation of q in Eq. 13, were determined by atomic calculations (non-relativistic) for each configuration obtained from the MO calculations.

4 RESULTS AND DISCUSSION

4.1 Electronic structure

Molecular Orbital calculations were performed for the $[Ir(CN)_5]^{3-}$, $[Ir(CN)_5C\ell]^{4-}$ and $[Ir(CN)_4C\ell_2]^{4-}$ complex ions. Inter-atomic distances between metal and cyanide ions were estimated by extrapolation of values known for other transition metal hexacyano complexes or by sums of covalent radii. The metal-chlorine distance taken to be half the lattice parameter, unless otherwise specified. This corresponds to the distance between the $C\ell^-$ and the cation in the alkali chloride host. The values are: Ir-C=2.00 Å, C-N=1.16 Å, Ir-Cℓ = 2.814 Å (NaCℓ), 3.140 Å (KCℓ), 3.286 Å (RbCℓ host lattice).

A distance approximately equal to the sum of the Ir and Cℓ covalent radii was also adopted. Since experimentally there is no way to determine wether the Cℓ atom is placed at the proper lattice site or at shorter Ir-Cℓ distances, we consider both possibilities in the calculations. In Fig. 1 are depicted the complexes studied.

The metal ion is expected to lie out of the plane of the equatorial ligands in the penta-cyano and mono-chlorinated species (see Fig.1), as evidenced by EPR measurements[2]. Calculations for the energy defined as

$$E = \sum_i n_i e_i \ , \qquad (14)$$

which is the sum of the Molecular Orbital energies e_i multiplied by their occupation n_i, were carried out for several values of the angle θ between the principal symmetry axis of the complex and the equatorial Ir-CN bond. This quantity is expected to behave approximately in the same manner as the total energy of the molecule, when a structural parameter such as the angle θ is varied[32]. Figure 2 shows the energy E for the pentacyano complex as a function of θ. There is clearly a minimum for $\theta = 101{,}5^0$. This value is close to that found for the square pyramidal $[Ni(CN)_5]^{3-}$ complex by X-ray diffraction methods[33]. For $[Ir(CN)_5C\ell]^{4-}$, we observe two minima, one at $\theta < 90^0$ and another at $\theta > 90^0$. The first dominates at small Ir-Cℓ distances ($\sim 2.5\mathring{A}$) and the second at larger distances, as those corresponding to the metal-chloride distance in the host lattice. A third, less pronounced, energy minimum is observed at even larger distances. Figs. 3a and 3b illustrate what we have described. The exact angles at which the minima occur vary slightly with distance, and are given in the Tables. The existence of two stable bond lengths for a me-

tal-ligand bond in a transition metal complex has been acknowledged for some time, and is known as "bond-stretch isomerism"[34].

In Fig. 4 are shown the energy levels diagrams for the Molecular Orbitals of $[Ir(CN)_5]^{3-}$, $[Ir(CN)_5C\ell]^{4-}$ and $[Ir(CN)_4C\ell_2]^{4-}$. The "crystal field" levels, that is, the levels of large 5d character, are $2b_2$, 5e, $4a_1$ and $3b_1$ for $[Ir(CN)_5]^{3-}$, $2b_2$, 6e, $6a_1$ and $3b_1$ for $[Ir(CN)_5C\ell]^{4-}$ and $3e_g$, $2b_{2g}$, $4a_{1g}$ and $2b_{1g}$ for $[Ir(CN)_4C\ell_2]^{4-}$. The ordering $b_2 < e$ found for the pentacyano complexes with and without $C\ell$ is typical of square pyramidal coordination and is due to the fact that the metal atom is not located on the equatorial plane[35]. Overall, the MO levels scheme is rather similar in all three cases, except for the energy of the last occupied orbital ($4a_1$,$6a_1$ or $4a_{1g}$), which contains the paramagnetic electron. This is very low in $[Ir(CN)_5]^{3-}$, increases substantially in $[Ir(CN)_5C\ell]^{4-}$ and decreases again in $[Ir(CN)_4C\ell_2]^{4-}$.

As seen in Fig. 3b, the energy minimum for the small value of θ in $[Ir(CN)_5C\ell]^{4-}$ occurs at Ir-$C\ell$ distance smaller than 2.42Å. However, at distances smaller than this one an inversion of the $6a_1$ and $3b_1$ levels (HOMO and LUMO) occurs, and the paramagnetic electron occupies the $3b_1$ orbital. Since this is not evidenced by the EPR spectrum, which points to a $^2A_1$ ground state, it is likely that the isomer with a larger Ir-$C\ell$ distance is the one which actually occurs in the alkali halide crystals, being somehow stabilized by the lattice.

Table II gives the charge q on Ir, the total Mulliken-type populations for the complex ions, as well as the populations for the last occupied orbital. The charge on Ir is small and positive, and very similar in all cases, ranging from 0.22 to 0.29. The Ir configuration is nearer to d^8 than to the formal d^7, the 6s and 6p orbitals

having also non-negligible populations. π back-donation, however, is very small, as seen from the π^*(CN) populations. We believe that these actual numbers have become very small partly because of the weighted populations, which enhance large populations and suppress small ones. However, it is obvious that the π^*(CN) populations are small, independently of population definition. The weighted populations are also responsible for the π(CN) population having values unphysically higher than 4.00. Overall, the total populations are rather similar, differences being more noteworthy when we analyse the last occupied orbital, which contains the unpaired electron. In $[Ir(CN)_5]^{3-}$, this electron is distributed mainly between the $5d_{z^2}$ and $6p_z$ orbitals of Ir and the axial σ(CN). As a Cℓ ligand is attached, the unpaired electron leaves the Ir(6p) orbital and populates the Cℓ (3p). In summary, the unpaired electron is localized essentially on the principal molecular axis, for the distances considered.

As the Ir-Cℓ distance increases in $[Ir(CN)_5C\ell]^{4-}$, the distribution of the unpaired electron tends to resemble that in the pentacyano complex, becoming almost exactly the same for the Ir-Cℓ distance equal to 3.29Å, which is the metal-chlorine distance in RbCℓ.

4.2 Unpaired electron distribution

In Table III are given the calculated and experimental parameters which define the distribution of the paramagnetic electron over the orbitals of the atoms in the complexes. Also given in Table III are the equilibrium values for the angle θ between the axial and equatorial Ir-CN bonds in $[Ir(CN)_5]^{3-}$ and $[Ir(CN)_5C\ell]^{4-}$. Values were calculated for several Ir-Cℓ distances in $[Ir(CN)_5C\ell]^{4-}$ and

$[Ir(CN)_4C\ell_2]^{4-}$: 2.44Å (which is approximately the sum of the Ir-Cℓ ionic radii), 2.814Å (the Na-Cℓ distance in NaCℓ), 3.140Å (the K-Cℓ distance in KCℓ) and 3.286Å (the Rb-Cℓ distance in RbCℓ).

The comparison between calculated and experimental values is only approximate, since the definition itself of each parameter is not strictly the same in the theoretical and experimental frameworks. Bearing this in mind, we identify the $Ir(5d_{z^2})$ populations in the last occupied orbital with the experimentally-derived value of α^2 (see Section 2) and the populations $N_{ax}(2s)$, $N_{eq}(2s)$, etc., in this orbital with the parameters $f_s^{N,ax}$, $f_s^{N,eq}$, etc., as defined in Eq.(6) and Eq.(7).

First we notice that the lattice plays a role which is not limited to a variation of the Ir-Cℓ distance in the Cℓ-containing complexes. This is made clear by examining the α^2 values in $[Ir(CN)_5]^{3-}$ which vary noticeably with the lattice, even though Ir does not form a bond with Cℓ in this complex. We observe, however, the same trend in calculated and experimental α^2 values as the Metal-Chlorine distance is increased in $[Ir(CN)_5C\ell]^{4-}$, the same being true for $f_s^{C\ell}$ and $f_p^{C\ell}$. The overall agreement between theoretical and experimental values for $[Ir(CN)_5]^{3-}$ and $[Ir(CN)_5C\ell]^{4-}$ is fairly good, the only discrepancy being that the calculations overestimate the spin populations on the axial Nitrogen 2p orbital with respect to the equatorial.

For $[Ir(CN)_4C\ell_2]^{4-}$ the agreement is noticeably worse and the trends in α^2 and $f_p^{C\ell}$ with Ir-Cℓ distance are reverted. The explanation for this probably lies in the delocalization of electrons through the Ir-Cℓ bonds to the alkali metal ions in the lattice, for which

there is experimental evidence[6]. This same mechanism may explain the very small value of $f_p^{N,ax}$ found experimentally for the monochlorinated complex.

It must be noticed that since, these MO calculations are spin-restricted, only the unpaired electron on the last occupied orbital is considered in calculations of the spin distribution. In spin-unrestricted calculations, the polarization induced by this electron on the closed shells would be taken into account.

4.3 Electric field gradients

In Table IV are given the calculated and experimental values of the electric field gradient for the three complex ions studied.

The experimental values are only the absolute value of the EFG, since the sign was not measured. As explained in Section 3, the value Q = 0.78b for ^{193}Ir was employed in extracting the EFG from the Quadrupole Splittings[31]. Values of $\langle r^{-3}\rangle_{5d}$ (see Eq.13), obtained with local density atomic calculations, range from 10.18 to $10.26 a_0^{-3}$; values of $\langle r^{-3}\rangle_{6p}$ vary from 5.17 to $5.45\, a_0^{-3}$. In Table IV are also given 5d and 6p populations for $[Ir(CN)_5]^{3-}$; for $[Ir(CN)_5C\ell]^{4-}$ and $[Ir(CN)_4C\ell_2]^{4-}$, populations are given for only one Ir-Cℓ distance, as an example.

First we notice that all calculated values are negative, so we predict a negative V_{zz} for all three complexes. The 5d contribution dominates in all cases. The accord with experiment is fairly good for $[Ir(CN)_5]^{3-}$ and $[Ir(CN)_5C\ell]^{4-}$. For $[Ir(CN)_4C\ell_2]^{4-}$, calculated and experimental values are quite different. Again, this could be explained by the transfer of electrons to the lattice alkali ions in the latter complex[6].

The lattice plays a non-negligible role in the determination of the field gradient, as evidenced by the different experimental values obtained for $[Ir(CN)_5]^{3-}$ in NaCℓ, KCℓ and RbCℓ. In changing the Ir-Cℓ distance according to the lattice, we get the same trend as experiment for $[Ir(CN)_5C\ell]^{4-}$; however, the experimental variation is much greater, which shows that this is evidently not the only effect of the crystal.

The main mechanism which determines the sign and magnitude of V_{zz} in all cases is the larger total $5d_{z^2}$ populations, as compared to $5d_{x^2-y^2}$. These orbitals contribute with opposite signs (see Eq. 13 in Section 3). The 6p contribution is seen to be positive or negative, and is quite small for $[Ir(CN)_5]^{3-}$ and $[Ir(CN)_5C\ell]^{4-}$. For $[Ir(CN)_4C\ell_2]^{4-}$, it becomes large and positive, due to depletion of the $6p_z$ orbital. However, for this case a calculation is needed including atoms of the alkali halide crystals.

The mechanisms which produce the EFG in these complex ions are quite different from that in covalent complexes of Ru containing the ligand NO[13]. For these, back-donation to the ligand NO plays a dominant rôle, depleting the orbitals $4d_{xz(yz)}$ of Ru. In the present case, as seen in Section 4.1, back-donation to the CN ligand is small.

5 CONCLUSIONS

The semi-empirical method employed to perform Molecular Orbital calculations for the divalent paramagnetic complex ions $[Ir(CN)_5]^{3-}$, $[Ir(CN)_5C\ell]^{4-}$ and $[Ir(CN)_4C\ell_2]^{4-}$ has been proved to be quite useful in understanding their electronic structure. An interesting inversion of the angle $(CN)_{ax} - Ir - (CN)_{eq}$ in $[Ir(CN)_5C\ell]^{4-}$ was found when going from short to long Ir-Cℓ distances. The calculated distribution of the unpaired electron compares well with EPR data. A negative sign for the field gradient is predicted for all three complexes. The origin of the EFG is seen to be mainly a larger $5d_{z^2}$ population, with respect to $5d_{x^2-y^2}$. For $[Ir(CN)_4C\ell_2]^{4-}$, a calculation for a larger cluster is needed.

ACKOWLEDGEMENTS

The authors thank Professor M.C. Zerner for his interest and helpful discussions, and Professor P.T. Manoharan for sending part of the SCCC codes.

FIGURE CAPTIONS

Figure 1 - Iridium Complex Ions.

Figure 2 - Energy as a function of θ for $[Ir(CN)_5]^{3-}$.

a) Energy as defined in Eq. 14.

Figure 3a - Energy as a function of θ for $[Ir(CN)_5C\ell]^{4-}$.

a) Energy as defined in Eq. 14.

Figure 3b - Equal energy contours for $[Ir(CN)_5C\ell]^{4-}$. R is Ir-Cℓ distance.

Figure 4 - Molecular Orbital Energies for $[Ir(CN)_5]^{3-}$, $[Ir(CN)_5C\ell]^{4-}$ and $[Ir(CN)_4C\ell_2]^{4-}$.

a) Last occupied orbital, with one electron.

b) The orbital energies for Ir are the self-consistent VOIPs of $[Ir(CN)_5]^{3-}$. However, since the charges and configurations are similar, VOIPs of the other complexes are not very different.

TABLE CAPTIONS

Table I - Parameters for VOIP curves of Ir as a function of charge q $(VOIP = Aq^2 + Bq + C)^{(b)}$.

a) V.O. stands for valence orbital.

b) In units of $10^3 cm^{-1}$.

Table II - Mulliken-type populations for $[Ir(CN)_5]^{3-}$, $[Ir(CN)_5 C\ell]^{4-}$ and $[Ir(CN)_4 C\ell_2]^{4-}$.

a) CN and $C\ell$ populations are given per ligand. "Eq" stands for equatorial ligand, "ax" stands for axial.

Table III- Unpaired electron distribution[a].

a) See Sections 2 and 4.2 for definition of parameters.

b) Experimental values from Ref. (2). Values marked (*) are reported here for the first time.

Table IV- Electric field gradients, 5d and 6p Ir populations.

a) Experimental values from Refs. (36) and (37).

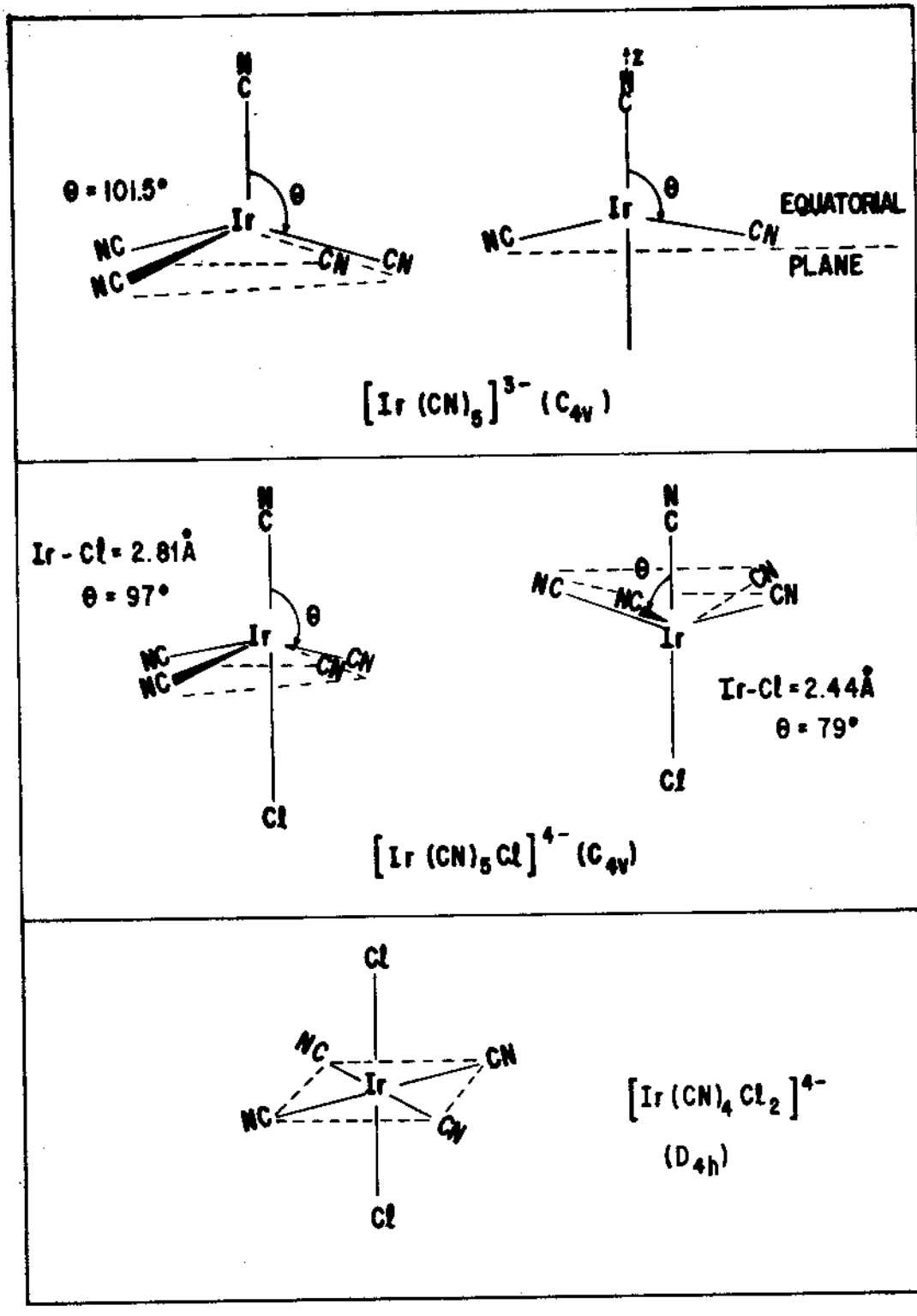
θ = 101.5°
θ
Ir
NC
NC
CN
CN
+z
EQUATORIAL
PLANE
[Ir (CN)5]3- (C4v)
Ir - Cl = 2.81Å
θ = 97°
Cl
Ir-Cl = 2.44Å
θ = 79°
[Ir (CN)5 Cl]4- (C4v)
[Ir (CN)4 Cl2]4-
(D4h)

Fig. 1

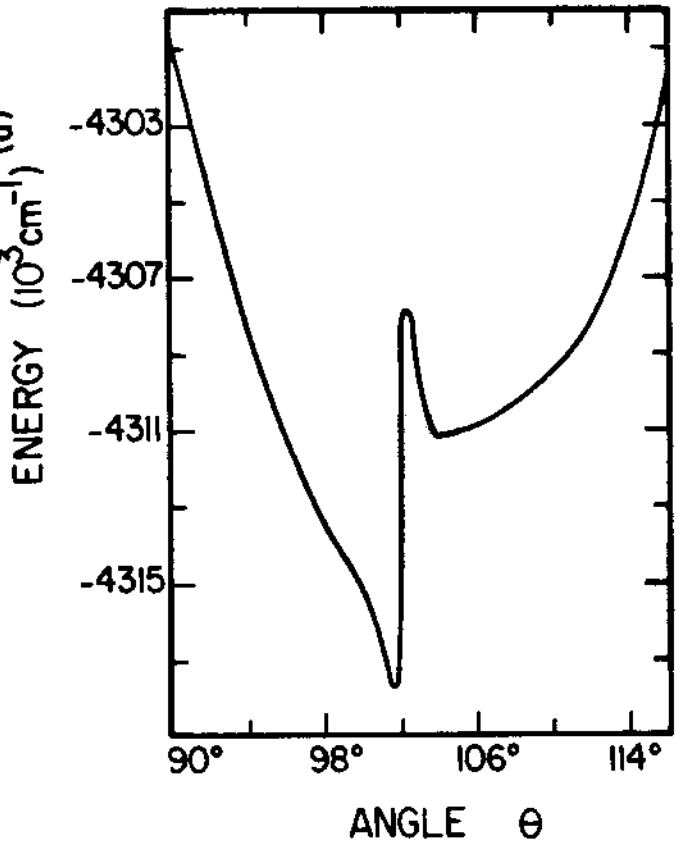

Fig. 2

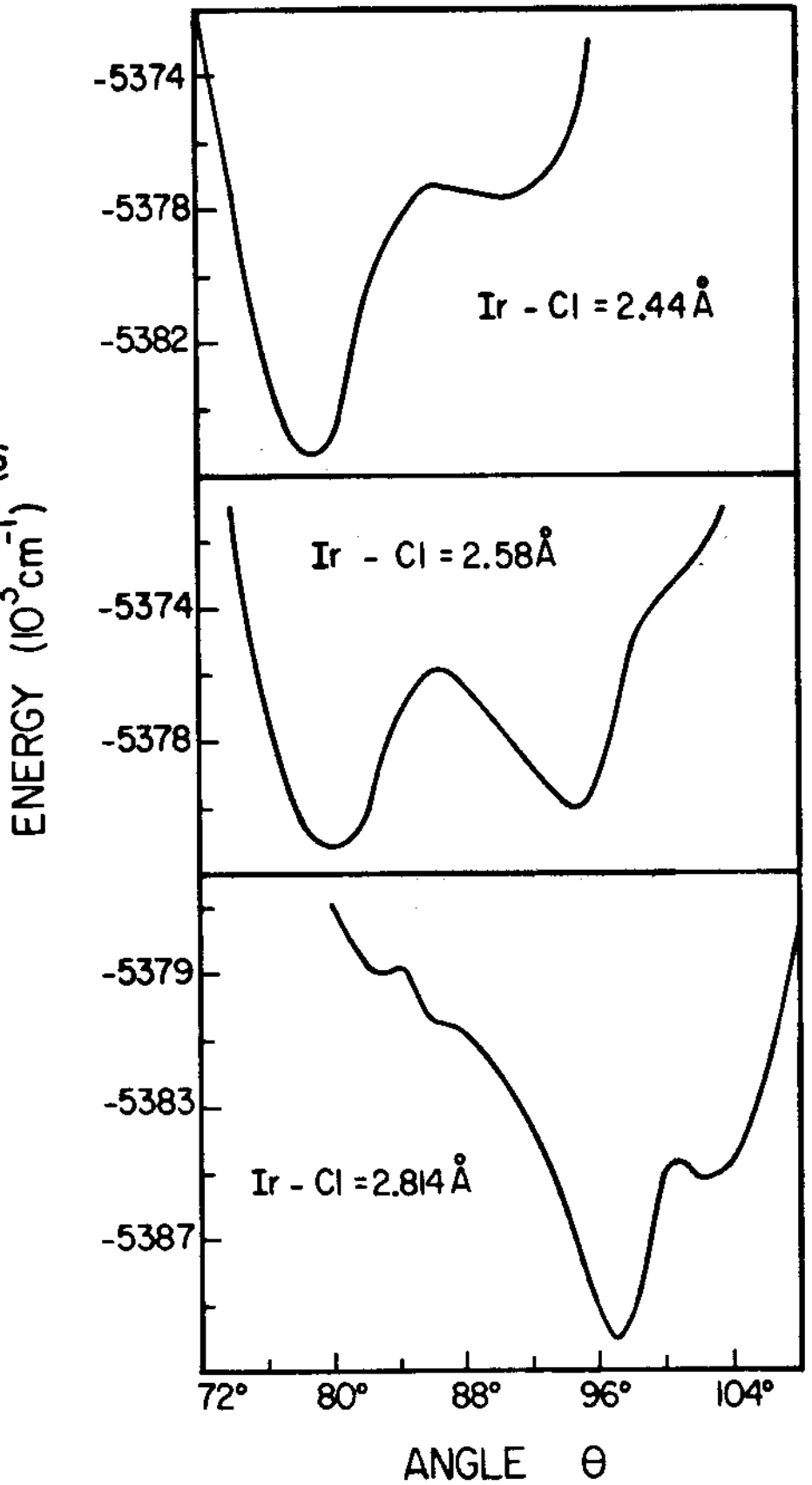
-5374
-5378
-5382
Ir - Cl = 2.44 Å
Ir - Cl = 2.58Å
-5374
-5378
-5379
-5383
Ir - Cl = 2.814 Å
-5387
ENERGY ($10^3 cm^{-1}$) (a)
72°
80°
88°
96°
104°
ANGLE θ

Fig. 3a

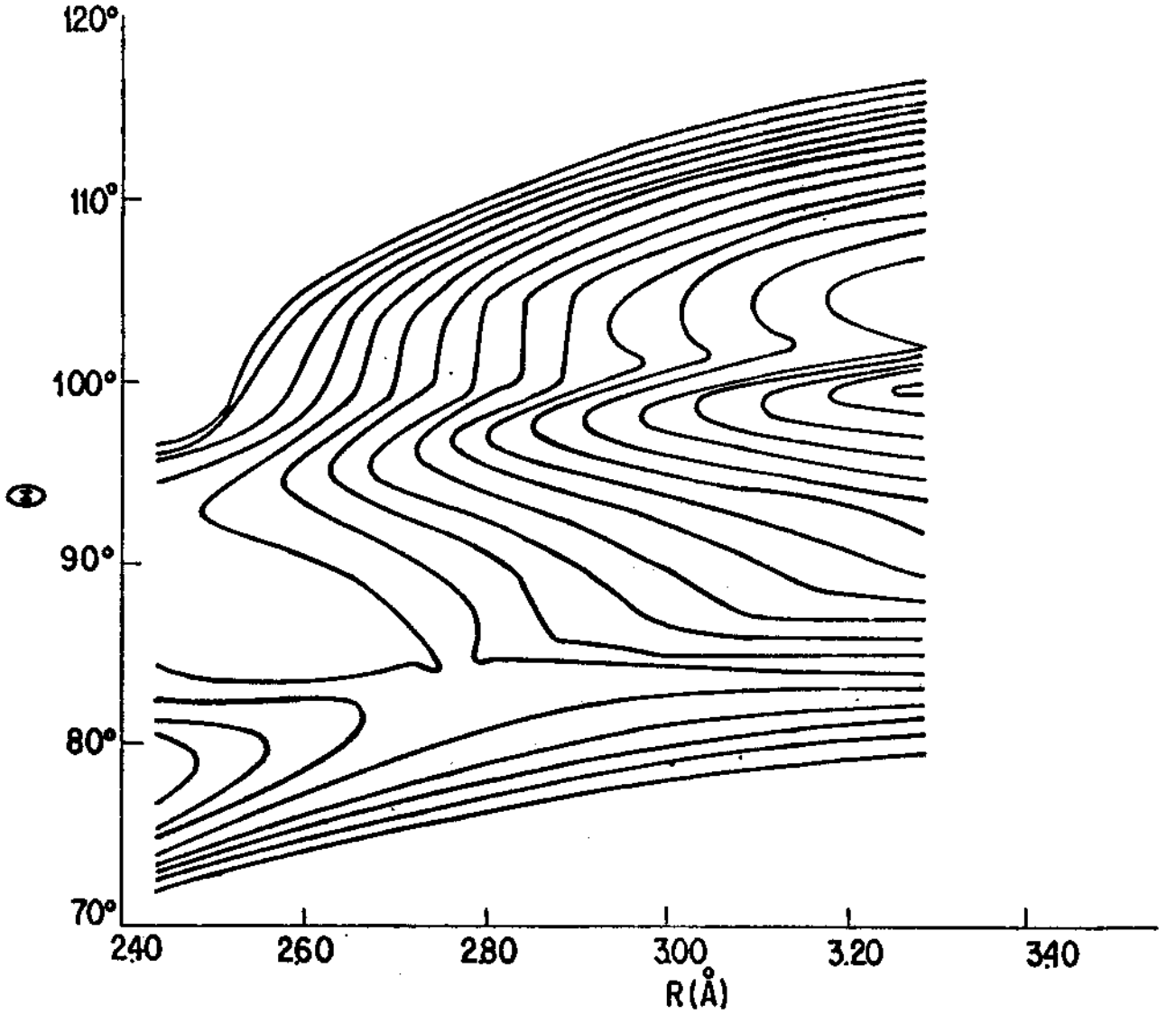

Fig. 3b

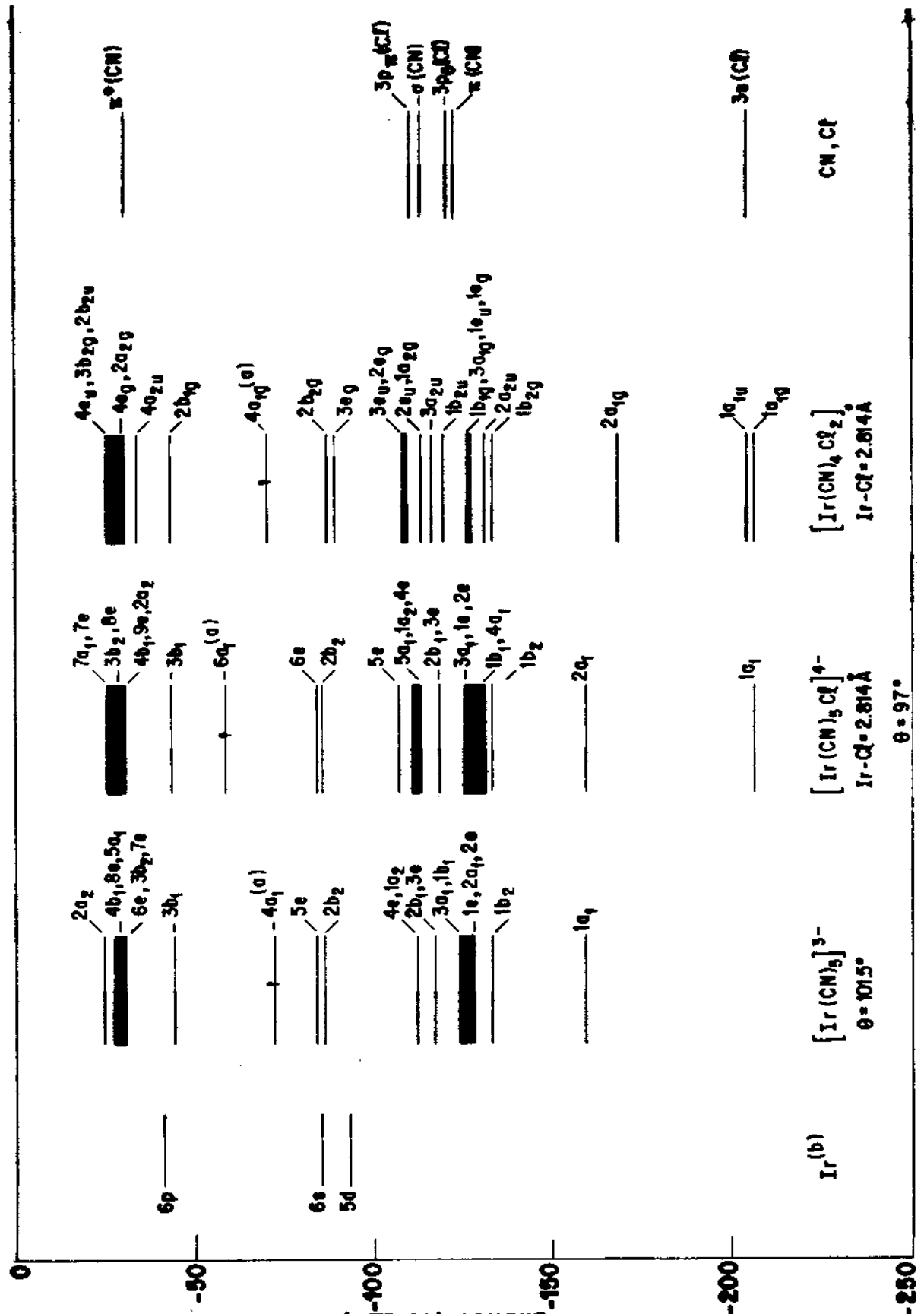
ENERGY (10³ cm⁻¹)
0
-50
-100
-150
-200
-250
Ir(b)
6p
6s
5d
[Ir(CN)5]3-
θ = 101.5°
[Ir(CN)5Cl]4-
Ir-Cl = 2.614Å
θ = 97°
[Ir(CN)4Cl2]2-
Ir-Cl = 2.614Å
CN, Cl
π*(CN)
3p(Cl)
σ(CN)
π(CN)
4a1, 3b2g, 2b2u
4b1g, 2a2g
4a2u
2b1g
4a1g(σ)
2b2g
3eg
3eu, 2a1g
2au, 1a2g
3a2u
1b2u
1b1g, 3a1g, 1eu, 1a1g
2a2u
1b2g
2a1g
1a1u
1a1g
7a1, 7e
3b2, 8e
4b1, 9a, 2a2
3b1
6a1(σ)
6e
2b2
5e
5a1, 1a2, 4e
2b1, 3e
3a1, 1e, 2e
1b1, 4a1
1b2
2a1
1a1
2a2
4b1, 8e, 5a1
6e, 3b2, 7e
3b1
4a1(σ)
5e
2b2
4e, 1a2
2b1, 3e
3a1, 1b1
1e, 2a1, 2e
1b2
1a1

Fig. 4

TABLE I

Configuration	V.O.[a]	A	B	C	Calculated VOIP (Ir^0)	Experimental VOIP (Ir^0)
$5d^9$	d	6.45	74.2	55.7	55.7	56.1
$5d^8 6s$	d	5.59	79.2	68.4		
$5d^8 6p$	d	6.37	76.9	78.9		
$5d^8 6s$	s	4.19	64.1	66.5	66.5	67.8
$5d^7 6s^2$	s	4.23	66.0	73.0		
$5d^7 6s6p$	s	4.76	64.0	80.5		
$5d^8 6p$	p	5.17	52.3	31.3		
$5d^7 6p^2$	p	4.76	55.1	40.2		
$5d^7 6s6p$	p	4.51	55.8	34.8		

TABLE II

Total Populations

Complex Ion	Ir-Cℓ distance (Å)	Ir			q	σ(CN)	π(CN)	π*(CN)	Cℓ(3s)	Cℓ(3p)
		5d	6s	6p						
$[Ir(CN)_5]^{3-}$	-	7.68	0.60	0.51	0.22	1.56	4.08	0.01	-	-
$[Ir(CN)_5Cℓ]^{4-}$	2.44	7.76	0.54	0.45	0.25	1.60	4.07	0.01	2.05	5.81
	2.814 (NaCℓ)	7.76	0.58	0.42	0.24	1.59	4.10	0.01	2.05	5.71
$[Ir(CN)_4Cℓ_2]^{4-}$	2.44	7.79	0.49	0.43	0.29	1.58	4.08	0.01	2.05	5.75
	2.814 (NaCℓ)	7.78	0.55	0.38	0.28	1.56	4.11	0.01	2.03	5.75

Populations of the last occupied orbital (a_1 or a_{1g})										
Complex Ion	Ir-Cℓ distance (Å)	Ir			$\sigma_{eq}(CN)^{(a)}$	$\sigma_{ax}(CN)$	$\pi_{eq}(CN)$	$\pi^*_{eq}(CN)$	Cℓ(3s)	Cℓ(3p)
		$5d_{z^2}$	6s	$6p_z$						
$[Ir(CN)_5]^{3-}$	-	0.52	0.01	0.17	0.02	0.19	0.01	0.0	-	-
$[Ir(CN)_5Cℓ]^{4-}$	2.44	0.46	0.0	0.01	0.04	0.21	0.0	0.01	0.02	0.09
	2.814 (NaCℓ)	0.50	0.0	0.05	0.03	0.19	0.0	0.0	0.01	0.10
$[Ir(CN)_4Cℓ_2]^{4-}$	2.44	0.51	0.0	-	0.05	-	-	-	0.03	0.12
	2.814 (NaCℓ)	0.62	0.02	-	0.03	-	-	-	0.01	0.12

TABLE III

Complex Ion			θ	α^2	$f_s^{N,ax}$	$f_p^{N,ax}$	$f_s^{N,eq}$	$f_p^{N,eq}$	f_s^{Cl}	f_p^{Cl}
$[Ir(CN)_5]^{3-}$	Calculated	-	101.5°	0.52	0.006	0.083	0.001	0.015	-	-
	(b) experimental	NaCl		0.53						
		KCl		0.50	0.009	0.050	0.001	0.052	-	-
		RbCl		0.47						
$[Ir(CN)_5Cl]^{4-}$	Calculated	Ir-Cl= 2.44Å	79°	0.46	0.007	0.094	0.001	0.022	0.018	0.094
		Ir-Cl= 2.814Å	97°	0.50	0.006	0.083	0.001	0.016	0.013	0.095
		Ir-Cl= 3.140Å	99°	0.51	0.006	0.081	0.001	0.015	0.005	0.056
		Ir-Cl= 3.286Å	100°	0.51	0.006	0.081	0.001	0.015	0.002	0.038
	(b) experinemtal	NaCl		0.5					0.013*	0.134*
		KCl		0.55	0.008	0.006	0.001*	0.041*	0.006	0.086
		RbCl		0.6						
$[Ir(CN)_4Cl_2]^{4-}$	Calculated	Ir-Cl= 2.44Å	-	0.51	-	-	0.002	0.021	0.029	0.123
		Ir-Cl= 2.814Å	-	0.62	-	-	0.001	0.012	0.011	0.115
		Ir-Cl= 3.140Å	-	0.72	-	-	0.0	0.004	0.004	0.092
		Ir-Cl= 3.286Å	-	0.76	-	-	0.0	0.002	0.003	0.078
	(b) experimental	NaCl	-	0.35	-	-			0.013	0.171
		KCl	-	0.18	-	-			0.012	0.175
		RbCl	-	0.21	-	-			0.011	0.187

TABLE IV

Complex Ion	Ir-Cℓ distance (Å)	θ	5d populations				6p Populations		V_{zz}(5d) (10^{17}V/cm^2)	V_{zz}(6p) (10^{17}V/cm^2)	Total V_{zz} (10^{17}V/cm^2)	Experimental $V_{zz}^{(a)}$ (10^{17}V/cm^2)
			$5d_{z^2}$	$5d_{x^2-y^2}$	$5d_{xy}$	$5d_{xz(yz)}$	$6p_{x(y)}$	$6p_z$				
$[Ir(CN)_5]^{3-}$	–	101.5°	1.242	0.936	1.869	1.815	0.154	0.201	-14.38	-1.92	-16.30	NaCℓ:25.10 KCℓ :21.29 RbCℓ:13.03
$[Ir(CN)_5Cℓ]^{4-}$	2.44	79°							-18.02	+1.98	-16.04	
	2.814	97°	1.290	0.912	1.866	1.847	0.141	0.135	-20.30	+0.24	-20.06	NaCℓ:30.51
	3.140	99°							-16.94	-0.95	-17.89	KCℓ :19.70
	3.286	100°							-15.83	-1.10	-16.93	RbCℓ:11.44
$[Ir(CN)_4Cℓ_2]^{4-}$	2.44	–							-16.54	+2.64	-13.90	
	2.814	–	1.194	0.941	1.863	1.894	0.161	0.054	-16.07	+4.41	-11.66	NaCℓ:67.69
	3.140	–							-11.31	+5.84	- 5.47	KCℓ:76.27
	3.286	–							- 8.85	+6.40	-2,45	RbCℓ:89.61

REFERENCES

1) A. Abragam and B. Bleaney, "Electron Paramagnetic Resonance of Transition Metal Ions", Clarendon Press, Oxford (1970).

2) N.V. Vugman and V.K. Jain, "Electron Paramagnetic Resonance Studies of Irradiated Single Crystals of Alkali Halides Doped with Cyanide Complexes of Co, Rh, Ir, Fe, Ru and Os. A Review", Revue Roumaine de Physique, in press.

3) N.V. Vugman, A.O. Caride and J. Danon, J. Chem. Phys. 59, 4418 (1973).

4) N.V. Vugman, A.M. Rossi and J. Danon, J. Chem. Phys. 68, 3152, (1978).

5) N.V. Vugman and N.M. Pinhal, Mol. Phys. 49, 1315 (1983).

6) N.M. Pinhal and N.V. Vugman, J. Phys. C 18, 6273 (1985).

7) S. Martins Jr. and N.V. Vugman, Chem. Phys. Letts. 141, 548 (1987).

8) B.R. McGarvey, J. Phys. Chem. 71, 51 (1967).

9) P.W. Atkins and M.C.R. Symons, "The Structure of Inorganic Radicals", Elsevier, Amsterdam (1967).

10) R.G. Hayes, "ESR of Metal Complexes", Ed. by Teh Fu Yen, Plenum Press, New York (1969), pg. 23.

11) C.J. Ballhausen and H.B. Gray, "Molecular Orbital Theory", Benjamin, New York (1965); C.J. Ballhausen and H.B. Gray, Inorg. Chem., 2, 426 (1963).

12) M. Wolfsberg and L. Helmholz, J. Chem. Phys. 20, 837 (1952).

13) D. Guenzburger, A. Garnier and J. Danon, Inorg. Chimica Acta, 21, 119 (1977).

14) H. Basch, A. Viste and H.B. Gray, J. Chem. Phys. 44, 10 (1966).

15) V.I. Baranoskii and A.B. Nikol'skii, Theoret. Exp. Chem. 3, 309 (1970).

16) I. Lindgren and A. Rosén, "Case Studies in Atomic Physics" 4, 93 (1974).

17) W. Kohn and L.J. Sham, Phys. Rev. 140, A1133 (1965); R. Gaspar, Acta Phys. Acad. Sci. Hung., 3, 263 (1954).

18) J.C. Slater, "Quantum Theory of Molecules and Solids", vol. IV, McGraw-Hill, New York (1974).

19) S.R. Nogueira and D. Guenzburger, unpublished.

20) L.L. Lohr Jr. and P. Pyykkö, Chem. Phys. Letters, 62, 333 (1979).

21) J. Chris Culbersom, P. Knappe, N. Rösch and M.C. Zerner, Theor. Chim. Acta 71, 21 (1987).

22) P.T. Manoharan and H.B. Gray, J. Am. Chem. Soc. 87, 3340 (1965).

23) J.J. Alexander and H.B. Gray, J. Am. Chem. Soc. 90, 4260 (1968); G.L. Geoffroy, M.S. Wrighton, G.S. Hammond and H.B. Gray, Inorg. Chem. 13, 430 (1974).

24) H. Basch and H.B. Gray, Theoret. Chim. Acta 4, 367 (1966).

25) E. Clementi, "Tables of Atomic Functions", Suppl. to "Ab-initio Computations in Atoms and Molecules", I.B.M. Journal of Research and Development, 9, 2 (1965).

26) R.S. Mulliken, J. Chem. Phys. 23, 1833 (1955).

27) J.J. Alexander and H.B. Gray, Coord. Chem. Rev. 2, 29 (1967).

28) R.M. Sternheimer, Phys. Rev. 164, 10 (1967).

29) D.E. Ellis, D. Guenzburger and H.B. Jansen, Phys. Rev. B28, 3697 (1985).

30) See, for example: S. Büttgenbach, M. Herschel, G. Meisel, E. Schrödl and W. Witte, Z. Physik 263, 341 (1973); W.J. Childs, M. Fred, E. Schrödl and Th. A.M. van Kleef, Phys. Rev. A10, 1028 (1973).

31) R. Vianden, Hyperfine Interactions 15/16, 1081 (1983).

32) R. Hoffman, J. Chem. Phys. 39, 1397 (1963).

33) K.N. Raymond, P.W.R. Corfied and J.A. Ibers, Inorganic Chemistry 7, 1362 (1968).

34) Y. Jean, A. Lledos, J.K. Burdett and R. Hoffmann, in press.

35) D. Guenzburger, A.O. Caride and E. Zuleta, Chem. Phys. Letters 14, 239 (1972).

36) N.M. Pinhal, Ph.D. Thesis, Universidade Federal do Rio de Janeiro (1986).

37) N.V. Vugman and N.M. Pinhal, Bull. Mag. Res. 2, 196 (1980).